

# Three-Dimensional Ordered CeO<sub>2</sub> Hollow Spheres (3DOHSs-CeO<sub>2</sub>) from Polymethylmethacrylate/CeO<sub>2</sub> Core/Shell Microsphere Colloidal Crystals

Ailian Chen<sup>1</sup> · Yang Chen<sup>2,3</sup> · Zhigang Chen<sup>3</sup>

Received: 11 July 2015 / Accepted: 14 September 2015 / Published online: 18 September 2015  
© Springer Science+Business Media New York 2015

**Abstract** The composite microspheres containing polymethylmethacrylate (PMMA) cores and ceria (CeO<sub>2</sub>) nanoparticles shells were synthesized by in situ chemical precipitation based on electrostatic interaction. The PMMA/CeO<sub>2</sub> colloidal crystal templates were self-assembled by a modified two-substrate vertical deposition method. After removal of the polymer cores by calcination, the three-dimensional ordered CeO<sub>2</sub> hollow spheres (3DOHSs-CeO<sub>2</sub>) films were fabricated. The resulting 3DOHSs-CeO<sub>2</sub> materials were characterized by X-ray diffraction, field emission scanning electron microscopy, high resolution transmission electron microscopy, and N<sub>2</sub> adsorption–desorption analysis. Results indicate that the obtained samples presented a typical face-centered cubic structure, and the CeO<sub>2</sub> hollow spheres (HSs) formed shared necks with each other. The average CeO<sub>2</sub> HSs diameters and center-to-center distances were 230–240 nm, and the porous shells (20–30 nm in thickness) of CeO<sub>2</sub> HSs were consisted of tiny CeO<sub>2</sub> nanoparticles with a size of 10–20 nm. This work suggested that the 3DOHSs architectures would be valuable for photonic crystals, advanced optical and catalytic applications.

**Keywords** Colloidal crystal · Ceria · Hollow sphere · Three-dimensional ordered architecture

## 1 Introduction

Ceria (CeO<sub>2</sub>) materials with a cubic fluorite-type crystallographic symmetry has attracted much attention due to their potential applications in photocatalysts, fuel cells, heterogeneous catalysts, polishing abrasives, and UV absorbers [1–3]. Many efforts have been devoted to improving the performance of CeO<sub>2</sub> materials through structural and morphological control, including nano-particles [3, 4], nano-wires [5, 6], nano-rods [7], nano-tubes [8], nano-plates [9], nano-spheres [10], nano-cubes [2, 11], nano-films [12], nano-octahedrons [13, 14], and hollow spheres [15].

Three-dimensionally (3D) ordered inorganic materials have attracted great interests for numerous applications in photonic devices, catalysis, sensors, batteries, supercapacitors, fuel cells, sorption, and thermal insulation [16]. The conventional approach is the hard-templating process with colloidal crystals as the sacrificial templates. Up to date, 3D ordered CeO<sub>2</sub> materials are mainly focused on 3D ordered macroporous (3DOM) products or inverse opals due to their bicontinuous nanostructure (a continuous nanostructured framework with large interfacial area and a 3D interconnected pore system). Waterhouse et al. [17] fabricated inverse opal ceria films and powders, exhibiting 3DOM structures and a photonic band gap in the visible region using a colloidal crystal template approach. The obtained 3DOM-CeO<sub>2</sub> powders showed an improved thermal stability compared to non-networked CeO<sub>2</sub> nanoparticles of comparable initial crystallite size and surface area. Liu et al. [18] also prepared 3DOM-

✉ Yang Chen  
cy.jpu@126.com

<sup>1</sup> School of Mechanical Engineering, Changzhou University, Changzhou 213164, Jiangsu, China

<sup>2</sup> School of Materials Science and Engineering, Changzhou University, Changzhou 213164, Jiangsu, China

<sup>3</sup> Jiangsu Key Laboratory for Environment Functional Materials, Suzhou University of Science and Technology, Suzhou 215009, Jiangsu, China

CeO<sub>2</sub> materials with hierarchical pore structure via a dual hard-soft templating strategy. Compared to conventional bulk CeO<sub>2</sub> materials, the hierarchical 3DOM-CeO<sub>2</sub> supported iridium catalysts exhibited an enhanced catalytic activity in CO oxidation.

Colloidal crystal templates method can also be applied in fabrication of 3D ordered inorganic hollow spheres (3DOHSs). Marlow et al. [19] demonstrated a method to coat a uniform vinyl-SiO<sub>2</sub> shell on negatively charged polystyrene particles. The core-shell hybrids were self-assembled into colloidal crystals using a capillary deposition method, and then converted into 3DOHSs-SiO<sub>2</sub> films by calcination. Dinh et al. [20] reported a novel Au/TiO<sub>2</sub> nanostructured photocatalyst, which was constructed by the 3D ordered assembly of thin-shell Au/TiO<sub>2</sub> hollow nanospheres. The novel 3DOHSs-Au/TiO<sub>2</sub> photocatalysts exhibited an improved photocatalytic activity for the photocatalytic decomposition of isopropanol under visible-light illumination by comparison with than conventional Au/TiO<sub>2</sub> nanopowders. In our previous work [21], high-quality 3D ordered TiO<sub>2</sub> hollow-spheres films were fabricated using polystyrene spheres colloidal crystals as sacrificial templates and titanium tetrachloride as titanium sources. To the best of our knowledge, there are few reports on the fabrication of 3DOHSs-CeO<sub>2</sub> materials using colloidal crystal templates.

Herein, we synthesized well-defined core-shell structured polymethylmethacrylate (PMMA)/CeO<sub>2</sub> composites, and PMMA/CeO<sub>2</sub> microspheres colloidal crystals were obtained via a modified two-substrate vertical deposition method [22, 23]. After removal of PMMA cores by calcination, 3DOHSs-CeO<sub>2</sub> materials with well-ordered periodicity were obtained. A detailed structural characterization of the as-prepared samples indicated the CeO<sub>2</sub> hollow spheres (HSs) exhibited a face-centered cubic packing structure, and the CeO<sub>2</sub> HSs were connected with shared necks.

## 2 Experimental Section

### 2.1 Materials

Methyl methacrylate (MMA) was obtained from Shanghai Lingfeng Chemical Reagent Co. (China) and purified with an inhibitor removal column. Ammonia (25–28 wt%), poly(sodium-*p*-styrene-sulfonate) (PSS), sodium chloride (NaCl), potassium persulfate (KPS), absolute ethanol, hexamethylenetetramine (HMT), and cerium nitrate hexahydrate (Ce(NO<sub>3</sub>)<sub>3</sub>·6H<sub>2</sub>O) were purchased from Shanghai Chemical Reagent Co. (China) and used as received.

### 2.2 Preparation of PMMA/CeO<sub>2</sub> Composite Microspheres

Monodisperse PMMA spheres were synthesized by a modified soap-free emulsion polymerization [24]. Typically, 8 g of MMA and 150 g of deionized (DI) water were charged into a 250 mL round bottom flask equipped with a Graham condenser, magnetic stirrer, and thermometer with a temperature controller. The mixture was heated to 70 °C at a stirring rate of 250 rpm for 2 h, and then injected by the mixture of 0.2 g KPS and 30 g DI water to initiate polymerization. The polymerization was continued at the same temperature for another 7 h.

For the preparation of PMMA/CeO<sub>2</sub> microspheres, 4 mL PMMA colloids, Ce(NO<sub>3</sub>)<sub>3</sub>·6H<sub>2</sub>O (1.5 g) and HMT (2.4 g) were charged into 200 mL DI water. The mixture was stirred for 10 min to form homogeneous suspension. Subsequently, the mixture was reacted at 75 °C for 2 h. These operations were performed under constant magnetic stirring at 200 rpm. The resulting precipitates were centrifuged, washed with DI water and absolute ethanol, and dried at 80 °C.

### 2.3 Surface Modification of PMMA/CeO<sub>2</sub> Composites with PSS

According to the literature [25], NaCl (1.7 g) and PSS (0.2 g) were charged into the 40 mL PMMA/CeO<sub>2</sub> suspensions (3 wt%), the mixture was stirred at room temperature for 2 h. Subsequently, the particles were collected by centrifugation and washed with DI water three times to ensure removal of residual polyelectrolyte and salt. Finally, the PSS-stabilized PMMA/CeO<sub>2</sub> composites were obtained, and dispersed in DI water for self-assembly.

### 2.4 Fabrication of PMMA/CeO<sub>2</sub> Colloidal Crystals and 3DOHSs-CeO<sub>2</sub>

The PMMA/CeO<sub>2</sub> colloidal crystals were obtained by a modified two-substrate vertical deposition [26] through electrostatic colloid stabilization by adsorption of PSS on the surface of PMMA/CeO<sub>2</sub> composites. Oxidized silicon wafers and glass slides (10 × 25 mm<sup>2</sup>) were boiled in the piranha solution (3:1 v/v 98 % H<sub>2</sub>SO<sub>4</sub>/35 % H<sub>2</sub>O<sub>2</sub>) at 60 °C for 1 h to create a clean hydrophilic surface. A piece of pretreated oxidized silicon wafer and cover glass were vertically placed together and then dipped into the PMMA/CeO<sub>2</sub> composites suspension (3.0 wt%). In the process of the evaporation of the solvent, the microspheres self-assembled to form ordered colloidal crystals under induction of the capillary force. Subsequently, the cover glass

was peeled off carefully after the colloidal crystals were dried completely. Finally, the colloidal crystals on the oxidized silicon wafer were calcinated at 500 °C (1 °C/min) for 2 h to remove the PMMA templates, subsequently formed 3D ordered CeO<sub>2</sub> hollow spheres.

## 2.5 Characterization

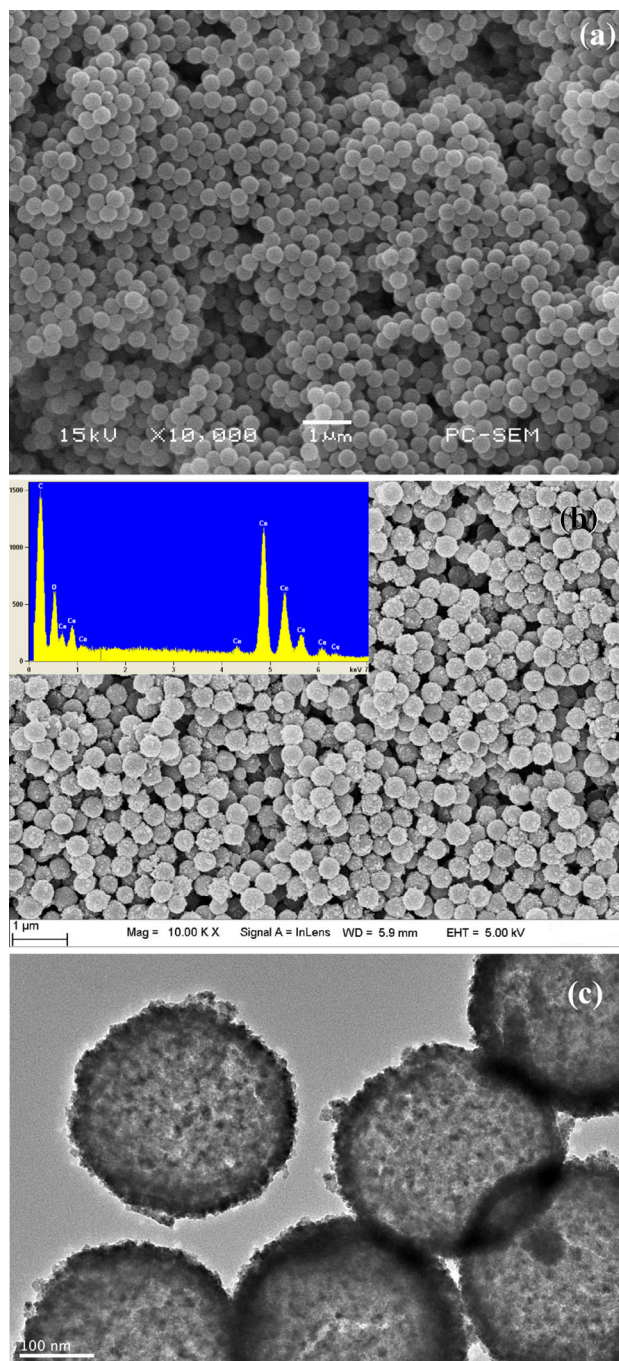
The crystal phases of the products were measured on a Rigaku D/Max 2500 PC X-ray diffractometer (XRD). The morphologies and composition of the samples were characterized using a JSM-6360LA scanning electron microscope (SEM), Hitachi S-4800 field emission SEM [equipped with an energy-dispersive X-ray spectrometer (EDS)], and a JEOL-2100 high-resolution transmission electron microscope [TEM, coupled with a selected area electron diffractometer (SAED)]. The surface area and the pore size of samples were determined using the Brunauer–Emmett–Teller (BET) model and the Barrett–Joyner–Halenda (BJH) method, respectively, derived from N<sub>2</sub> adsorption–desorption measurements performed on an automatic micropore physorption analyzer (Micromeritics ASAP 2020).

## 3 Results and Discussion

The morphologies and composition of the as-prepared PMMA and PMMA/CeO<sub>2</sub> particles are displayed in Fig. 1. As shown in Fig. 1a, the monodisperse PMMA colloids exhibit a uniform size of 250 nm with a deviation <5%. After coating, the PMMA/CeO<sub>2</sub> samples (Fig. 1b) are large-scale uniform spheres similar to the PMMA cores. Furthermore, the surfaces of the composites are much rough, indicating that the CeO<sub>2</sub> particles have been coated on the surfaces of PMMA cores. According to the EDS spectrum (inset in Fig. 1b), the surfaces of the composites consist of Ce, O and C elements. As confirmed by the TEM image of the composites (Fig. 1c), CeO<sub>2</sub> nanoparticles are uniformly immobilized on PMMA colloids. The strawberry-like PMMA/CeO<sub>2</sub> microspheres exhibit a well-defined core–shell structure. A possible mechanism for the formation of PMMA/CeO<sub>2</sub> microspheres is described in our previous work [27].

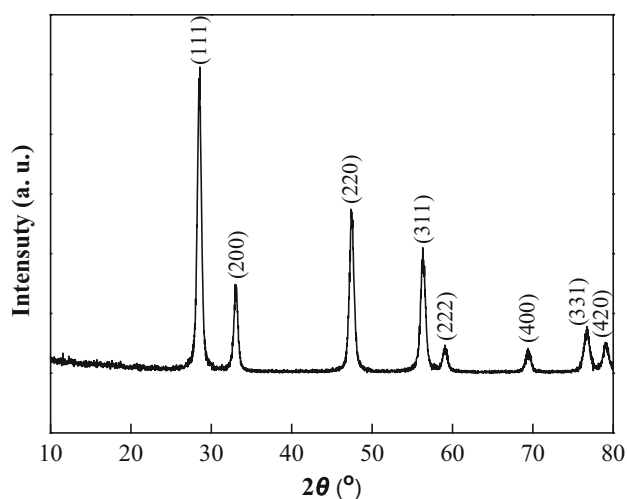
The XRD pattern of the 3DOHSs-CeO<sub>2</sub> products (Fig. 2) is indexed to the CeO<sub>2</sub> fluorite structure (space group = *Fm*3*m*, JCPDS card #34-0394) [2]. The characteristic XRD peaks located at different 2θ values matched well with the corresponding *hkl* planes of bulk CeO<sub>2</sub>. No additional impurity was found in the pattern, implying the high purity of the product. The average grain size determined by the Scherrer formula of CeO<sub>2</sub> powders was ca. 9.7 nm.

Figure 3 shows the representative FESEM images of the 3DOHSs-CeO<sub>2</sub> samples. The top-view image (Fig. 3a)



**Fig. 1** SEM (a, b), TEM (c) images and EDS spectrum (*inset*) of the obtained PMMA colloids and PMMA/CeO<sub>2</sub> composites

indicates that the products present a typical face-centered cubic packing structure with (111) plane parallel to the substrate. The average sphere diameters and center-to-center distances were 230–240 nm, which was determined by the high-magnification FESEM image (Fig. 3b). From the cross-section image (Fig. 3c), some holes could be clearly observed on the surfaces, indicating the hollow structure of CeO<sub>2</sub> spheres. And the films over ten layers of

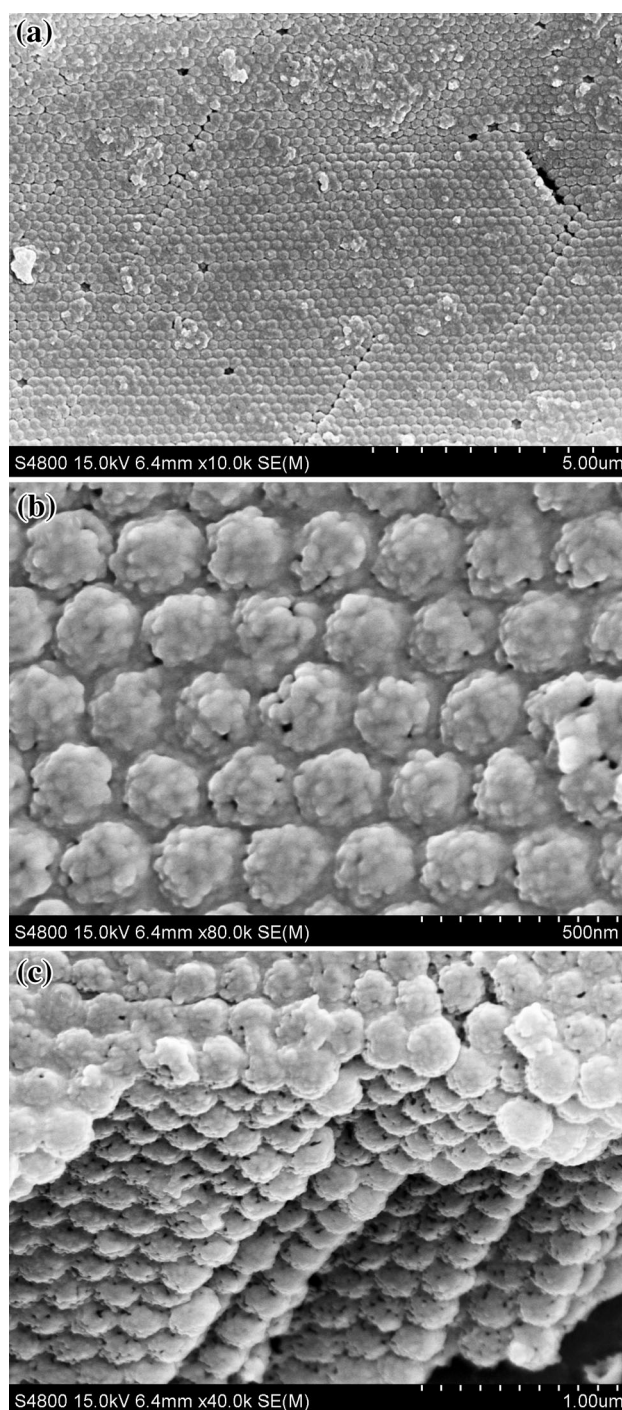


**Fig. 2** XRD pattern of the 3DOHSs-CeO<sub>2</sub> samples

CeO<sub>2</sub> hollow sphere arrays are formed. Furthermore, these hollow spheres are connected with shared necks, and the highly 3D ordered structure of CeO<sub>2</sub> hollow spheres are obtained after removing the PMMA cores of the hybrids colloidal crystals by calcination at 500 °C.

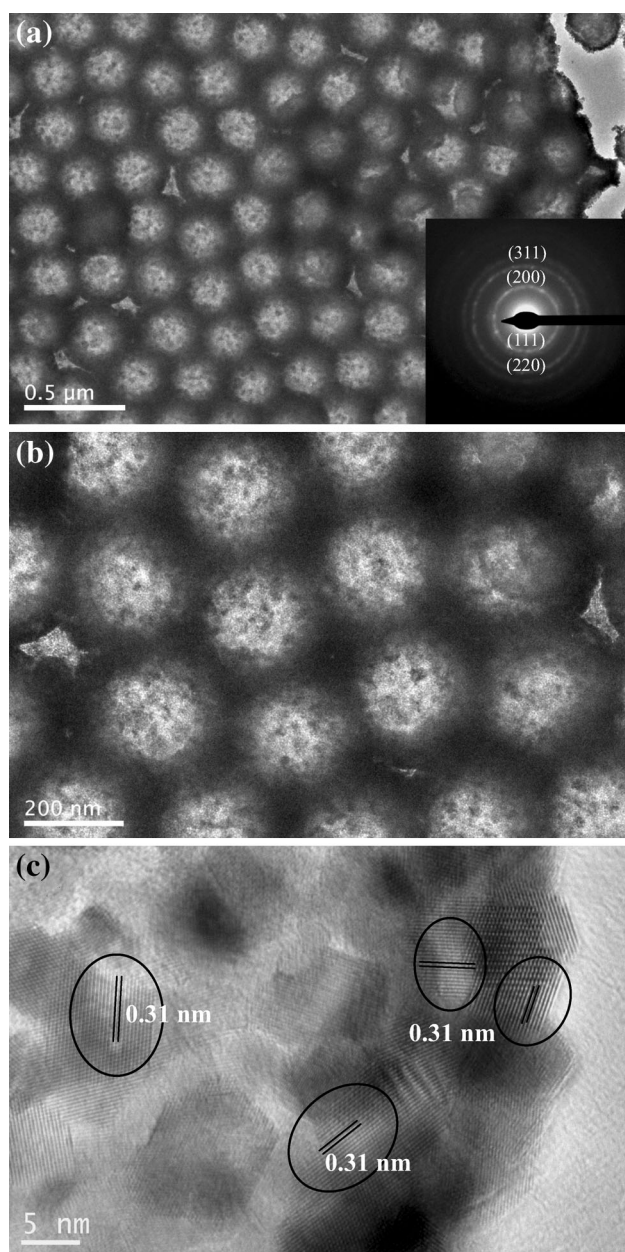
The structural details of the 3DOHSs-CeO<sub>2</sub> samples were further investigated by HRTEM and SAED analyses, and the representative results are illustrated in Fig. 4. The low-magnified TEM image (Fig. 4a) also confirms that the samples are consisted of closely packed, hexagonal array of CeO<sub>2</sub> hollow spheres. Furthermore, the SAED pattern of as-synthesized samples (inset in Fig. 4a) reveals the pure crystalline nature of as-synthesized particles with cubic fluorite structure, where (111), (200), (220) and (311) lattice planes were clearly indexed [28]. As confirmed by the high-magnified TEM image (Fig. 4b), the walls of CeO<sub>2</sub> hollow spheres are composed of small nanoparticles (10–20 nm), and the shell thickness is 20–30 nm. The CeO<sub>2</sub> HSs exhibited loose state and even some interparticle voids could be clearly observed. According to the HRTEM analysis, the measured interplanar distances of 0.31 nm achieved from the circled region in Fig. 4c are in correspondence with the lattice spacing of the (111) plane of CeO<sub>2</sub> [29].

Figure 5 shows the N<sub>2</sub> adsorption–desorption isotherms and the corresponding pore-size distribution curves (inset) of the 3DOHSs-CeO<sub>2</sub> products. The samples present isotherms of type IV, indicating the presence of mesopores (2–50 nm) [30]. The shapes of hysteresis loops are type H3 at a high relative pressure range of 0.8–1.0, indicating the presence of slit-like pores. The isotherms show high absorption at high relative pressure (P/P<sub>0</sub>) range (approaching 1.0), implying the formation of large mesopores and macropores [31]. The specific



**Fig. 3** SEM images and EDS spectrum (*inset*) of the 3DOHSs-CeO<sub>2</sub> samples: **a**, **b** top view image, **c** cross-section image

surface area determined by BET model is 84.61 m<sup>2</sup>/g. The pore size distribution curve (inset in Fig. 5) calculated from the desorption branch based on the BJH method is a wide range of 2–10 nm, further confirming the presence of mesopores. It is noted that more macroporous



**Fig. 4** TEM (a, b), HRTEM (c) images and SAED pattern (*inset*) of the 3DOHSs-CeO<sub>2</sub> samples

information (larger than 100 nm) cannot be directly obtained by N<sub>2</sub> adsorption–desorption analyses [32]. However, the hollow structures are clearly observed by cross-sectional FESEM image of the sample (Fig. 3c). Therefore, the results of FESEM, HRTEM and N<sub>2</sub> adsorption–desorption analysis reveal that the as-prepared 3DOHSs-CeO<sub>2</sub> materials possess a hierarchically multi-modal pore-size distribution from mesopores to macro pores.

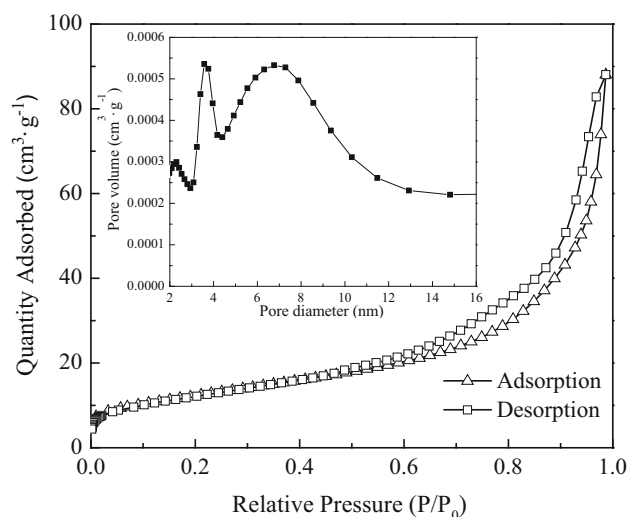


**Fig. 5** Nitrogen adsorption–desorption isotherms and pore size distribution (*inset*) of the as-synthesized 3DOHSs-CeO<sub>2</sub> samples

## 4 Conclusions

PMMA polymer cores were uniformly coated with CeO<sub>2</sub> nanoparticles, and well-defined core–shell structured PMMA/CeO<sub>2</sub> composite particles were obtained. The PMMA/CeO<sub>2</sub> composites colloidal crystals were fabricated through a modified two-substrate vertical deposition method. The three-dimensional ordered CeO<sub>2</sub> hollow spheres (3DOHSs-CeO<sub>2</sub>) were obtained by calcination to remove PMMA cores. Colloidal crystal templating is a simple and efficient method for the fabrication of the films composed of a closely packed, hexagonal array of the CeO<sub>2</sub> HSs without complicated apparatuses and procedures. These films will be important for promising applications in photonic crystals, advanced optical and catalytic materials. This method may provide an alternative to the fabrication of other high-quality 3D ordered inorganic HSs.

**Acknowledgments** The work was supported financially by the Applied Basic Research Project of Suzhou City (SYG201316) and the Key Laboratory for Environment Functional Materials of Jiangsu Province (SJHG1302).

## References

1. P. Pal, R.K. Singha, A. Saha, R. Bal, A.B. Panda, Defect-induced efficient partial oxidation of methane over nonstoichiometric Ni/CeO<sub>2</sub> nanocrystals. *J. Phys. Chem. C* **119**, 13610–13618 (2015)
2. K. Deori, D. Gupta, B. Saha, S. Deka, Design of 3-dimensionally self-assembled CeO<sub>2</sub> nanocube as a breakthrough catalyst for efficient alkylarene oxidation in water. *ACS Catal.* **4**, 3169–3179 (2014)

- Y. Lin, Z. Wu, J. Wen, K.R. Poepplmeier, L.D. Marks, Imaging the atomic surface structures of CeO<sub>2</sub> nanoparticles. *Nano Lett.* **14**, 191–196 (2014)
- L.E. Barton, M. Auffan, L. Olivi, J. Bottero, M.R. Wiesner, Heteroaggregation, transformation and fate of CeO<sub>2</sub> nanoparticles in wastewater treatment. *Environ. Pollut.* **203**, 122–129 (2015)
- Y. Li, X. Dong, J. Gao, D. Hei, X. Zhou, H. Zhang, A highly sensitive  $\gamma$ -radiation dosimeter based on the CeO<sub>2</sub> nanowires. *Physica E* **4**, 11550–11553 (2009)
- X. Lu, X. Li, J. Qian, Z. Chen, The surfactant-assisted synthesis of CeO<sub>2</sub> nanowires and their catalytic performance for CO oxidation. *Powder Technol.* **239**, 415–421 (2013)
- Y. Chen, T. Liu, C. Chen, W. Guo, R. Sun, S. Lv, M. Saito, S. Tsukimoto, Z. Wang, Synthesis and characterization of CeO<sub>2</sub> nano-rods. *Ceram. Int.* **39**, 6607–6610 (2013)
- J. Wu, J. Wang, Y. Du, H. Li, Y. Yang, X. Jia, Chemically controlled growth of porous CeO<sub>2</sub> nanotubes for Cr(VI) photoreduction. *Appl. Catal. B: Environ.* **174–175**, 435–444 (2015)
- H. Lin, C. Wu, R. Chiang, Facile synthesis of CeO<sub>2</sub> nanoplates and nanorods by [100] oriented growth. *J. Colloid Interface Sci.* **341**, 12–17 (2010)
- M. Zabilskiy, P. Djinović, B. Erjavec, G. Dražić, A. Pintar, Small CuO clusters on CeO<sub>2</sub> nanospheres as active species for catalytic N<sub>2</sub>O decomposition. *Appl. Catal. B* **163**, 113–122 (2015)
- Y.C. Zhang, M. Lei, K. Huang, C. Liang, Y.J. Wang, S.S. Ding, R. Zhang, D.Y. Fan, H.J. Yang, Y.G. Wang, A facile route to mono-dispersed CeO<sub>2</sub> nanocubes and their enhanced photocatalytic properties. *Mater. Lett.* **116**, 46–49 (2014)
- Y. Lu, S. Cai, Y. Liang, C. Bai, Z. Liu, Y. Guo, C. Cai, The mechanism of the nano-CeO<sub>2</sub> films deposition by electrochemistry method as coated conductor buffer layers. *Physica C* **512**, 1–5 (2015)
- X. Lu, X. Huang, S. Xie, D. Zheng, Z. Liu, C. Liang, Y. Tong, Facile electrochemical synthesis of single crystalline CeO<sub>2</sub> octahedrons and their optical properties. *Langmuir* **26**, 7569–7573 (2010)
- Q. Bo, F. Meng, L. Wang, Facile hydrothermal synthesis of CeO<sub>2</sub> nano-octahedrons and their magnetic properties. *Mater. Lett.* **133**, 216–219 (2014)
- Y. Chen, J. Xia, Facile fabrication of porous hollow CeO<sub>2</sub> microspheres using polystyrene spheres as templates. *J. Porous Mater.* **19**, 289–294 (2012)
- A. Stein, B.E. Wilson, S.G. Rudisill, Design and functionality of colloidal-crystal-templated materials—chemical applications of inverse opals. *Chem. Soc. Rev.* **42**, 2763–2803 (2013)
- G.I.N. Waterhouse, J.B. Metson, H. Idriss, D. Sun-Waterhouse, Physical and optical properties of inverse opal CeO<sub>2</sub> photonic crystals. *Chem. Mater.* **20**, 1183–1190 (2008)
- Z. Liu, X. Tan, C. Lv, Sucrose-assisted synthesis of three-dimensionally ordered macroporous CeO<sub>2</sub> and its use as a support for promotional catalytic performance of CO oxidation. *Appl. Surf. Sci.* **283**, 290–296 (2013)
- T. Deng, F. Marlow, Synthesis of monodisperse polystyrene@vinyl-SiO<sub>2</sub> core-shell particles and hollow SiO<sub>2</sub> spheres. *Chem. Mater.* **24**, 536–542 (2012)
- C. Dinh, H. Yen, F. Kleitz, T. Do, Three-dimensional ordered assembly of thin-shell Au/TiO<sub>2</sub> hollow nanospheres for enhanced visible-light-driven photocatalysis. *Angew. Chem. Int. Ed.* **53**, 6618–6623 (2014)
- Y. Chen, Z. Tang, Z. Chen, Facile fabrication and characterization of three-dimensional ordered films of TiO<sub>2</sub> hollow-spheres. *J. Inorg. Organomet. Polym.* **25**, 780–786 (2015)
- X. Chen, Z. Sun, Z. Chen, W. Shang, K. Zhang, B. Yang, Alternative preparation and morphologies of self-assembled colloidal crystals via combining capillarity and vertical deposition between two desired substrates. *Colloid Surf. A* **315**, 89–97 (2008)
- Z. Cai, J. Teng, Z. Xiong, Y. Li, Q. Li, X. Lu, X.S. Zhao, Fabrication of TiO<sub>2</sub> binary inverse opals without overlayers via the sandwich-vacuum infiltration of precursor. *Langmuir* **27**, 5157–5164 (2011)
- K. Shibuya, D. Nagao, H. Ishii, M. Konno, Advanced soap-free emulsion polymerization for highly pure, micron-sized, monodisperse polymer particles. *Polymer* **55**, 535–539 (2014)
- Y. Li, Z. Sun, J. Zhang, K. Zhang, Y. Wang, Z. Wang, X. Chen, S. Zhu, B. Yang, Polystyrene@TiO<sub>2</sub> core-shell microsphere colloidal crystals and nonspherical macro-porous materials. *J. Colloid Interface Sci.* **325**, 567–572 (2008)
- Z. Chen, T. Gang, Y. Wang, X. Chen, C. Guan, J. Zhang, Z. Sun, K. Zhang, B. Zhao, B. Yang, A simple method of preparing Ag nanoparticles coated silica colloidal crystals and polymer-Ag nanoparticles composite macroporous films. *Colloid Surf. A* **277**, 37–43 (2006)
- Y. Chen, Z. Li, N. Miao, Polymethylmethacrylate (PMMA)/CeO<sub>2</sub> hybrid particles for enhanced chemical mechanical polishing performance. *Tribol. Int.* **82**, 211–217 (2015)
- Q. Xie, Y. Zhao, H. Guo, A. Lu, X. Zhang, L. Wang, M. Chen, D. Peng, Facile preparation of well-dispersed CeO<sub>2</sub>-ZnO composite hollow microspheres with enhanced catalytic activity for CO oxidation. *ACS Appl. Mater. Interfaces* **6**, 421–428 (2014)
- K. Sato, M. Arai, J. Valmalette, H. Abe, Surface capping-assisted hydrothermal growth of gadolinium-doped CeO<sub>2</sub> nanocrystals dispersible in aqueous solutions. *Langmuir* **30**, 12049–12056 (2014)
- C.G.V. Burgess, D.H. Everett, S. Nuttall, Adsorption hysteresis in porous materials. *Pure Appl. Chem.* **61**, 1845–1852 (1989)
- J. Yu, G. Wang, B. Cheng, M. Zhou, Effects of hydrothermal temperature and time on the photocatalytic activity and microstructures of bimodal mesoporous TiO<sub>2</sub> powders. *Appl. Catal. B* **69**, 171–180 (2007)
- J. Yu, Q. Li, Z. Shu, Dye-sensitized solar cells based on double-layered TiO<sub>2</sub> composite films and enhanced photovoltaic performance. *Electrochim. Acta* **56**, 6293–6298 (2011)